LAWRENCE
LIVERMORE
NATIONAL
LABORATORY

UCRL-JRNL-211283

Uranus in 2003: Zonal Winds, Banded Structure, and Discrete Features

H. B. Hammel, I. de Pater, S. G. Gibbard, G. W. Lockwood, K. Rages

April 11, 2005

Icarus

Uranus in 2003: Zonal Winds, Banded Structure, and Discrete Features

H. B. Hammel[1,*], I. de Pater[2], S. Gibbard[3], G. W. Lockwood[4] , and K. Rages[5]

[1] Space Science Institute, Boulder, CO 80303, USA.

[2] Astronomy Department, University of California, Berkeley, CA 94720, USA.

[3] Lawrence Livermore National Laboratory, Livermore, CA 94550, USA.

[4] Lowell Observatory, Flagstaff, AZ 86001, USA.

[5] SETI Institute, Mountain View, CA 94043, USA.

To be submitted to *Icarus* on XX June 2004

Received _____

Corresponding Author.

Email address: hbh@alum.mit.edu

Manuscript Pages: 28

Figures: 4

Tables: 2

Running Title: Uranus in 2003

Editorial correspondence and proofs should be directed to:

Dr. Heidi B. Hammel
Space Science Institute
72 Sarah Bishop Road
Ridgefield, CT 06877

hbh@alum.mit.edu
203-438-3506

Abstract

Imaging of Uranus in 2003 with the Keck 10-m telescope reveals banded zonal structure and dozens of discrete cloud features at J and H bands; several features are also detectable at K'. By tracking features over four days, we extend the zonal wind profile well into the northern hemisphere. We report the first measurements of wind velocities at latitudes –13°, +19°, and northward of +43°, the first direct wind measurements near the equator, and the highest wind velocity seen yet on Uranus (+218 m/s). At northern mid-latitudes (+20° to +40°), the winds appear to have accelerated when compared to earlier HST and Keck observations; southern wind speeds (-20° to -43°) have not changed since Voyager measurements in 1986. The equator of Uranus exhibits a subtle wave structure, indicated by diffuse patches roughly every 30° in longitude. The largest discrete cloud features on Uranus show complex structure extending over tens of degrees, reminiscent of activity seen around Neptune's Great Dark Spot during the Voyager Encounter with that planet. There is no sign of a northern "polar collar" as is seen in the south, but a number of discrete features are seen at the appropriate latitudes; a northern collar may be in the early stages of development.

Keywords: Uranus, Atmosphere

1. Introduction

As Uranus approaches its 2007 equinox, much of its northern[1] hemisphere is receiving insolation for the first time in years (even decades at some latitudes), providing the first opportunity to study this hemisphere with modern astronomical equipment, and to study this planetary atmosphere as it experiences conditions of rapidly changing radiation balance. As discussed in Hammel and Lockwood (2004), Uranus appears to be undergoing significant seasonal change at multiple wavelengths. The observations presented here are part of a multi-year, multi-wavelength effort to characterize and understand these changes.

In this paper, we discuss near-infrared Adaptive Optics (AO) images of the Uranus system obtained in 2003. The AO system was optimized for planetary imaging (i.e., "closing the loop" on an extended source), resulting in Strehl ratios of 0.5 and spatial resolutions ≤0.05" for most of the data. The observations are presented in §2. We focus here on analyses of the planet's atmosphere (see Gibbard et al., 2004 for ring and satellite observations). Zonal wind measurements are in §3, and a discussion of hemispheric symmetry (or lack thereof at present) is found in §4. Complex horizontal structures associated with the largest discrete features are detailed in §5, with a final summary in §6.

---

[1] We adopt the IAU convention for "north," which means we have been viewing Uranus' *southern* hemisphere in sunlight for the past few decades.

2. Observations

We obtained images of the 3.7-arcsec diameter disk of Uranus on 3-6 October 2003 at three wavelengths using the 10-m William M. Keck II telescope on Mauna Kea, Hawaii, with the NIRC2 camera[2]. Our typical spatial resolution was 0.045-0.051 arcseconds (about 700 km at Uranus) on nearby stars at all wavelengths (filter characteristics are given in Table 2 of Gibbard et al., 2004). The atmospheric observations are summarized in Table 1. On the first night, two sets of data were taken; on the other nights we obtained three sets of images.

Table I [observation dates]

Figure 1 shows representative images from the sets, along with a schematic that identifies discrete features used to measure zonal wind velocities (see §3). Using the H-band images, which had the best S/N and smallest point-spread functions, we measured the discrete features' positions in pixel coordinates and then converted them to planetographic latitude and west longitude (defined such that the central meridian decreases with time) using an equatorial radius of 25559 km, oblateness of 0.023, pole positions α_o = 257.311 and δ_o = –15.175 (Davies et al., 1996), and the 17.24-hr radio rotation period (Ness et al., 1986; Warwick et al., 1986). To define

---

[2] The NIRC2 camera, a 1024x1024 Aladdin-3 InSb array, was designed by Keith Matthews and Tom Soifer, both of Caltech. It was built by Keith Matthews and engineer Sean Lin of Caltech, with help from James Larkin, Ian McLean, and others at UCLA (detector electronics, related software) and Al Conrad, Bob Goodrich, and Allan Honey at Keck Observatory (software). Jim Bell, Randy Campbell, and Drew Medeiros provided support in Waimea.

the planet center, we iteratively fit the illuminated limb of the planet on the basis of the brightness gradient near the limb. The accuracies of the codes for image navigation and feature position calculations have been verified by several independent groups (Hammel et al., 2001).

Figure 1 [representative images]

3. Zonal Winds of Uranus in 2003

In 2003, over three dozen features were seen in the H and J images, and 30 were seen on two or more nights (Fig. 1, Table 2). In comparison, ten features were tracked during the entire Voyager Encounter (Smith et al., 1986), five were tracked from Hubble Space Telescope (HST) near-infrared imaging in 1997 (Karkoschka, 1998), and thirteen trackable features were reported from other HST data taken over several years (Hammel et al., 2001). The large number of measurable features in 2003 and their distribution across the most of the planet's visible disk permitted a complete characterization of the zonal wind profile from southern to northern mid-latitudes (Fig. 2). A major advantage of our 2003 wind profile is its internal consistency: no ambiguity is introduced by combining diverse data sets obtained over many years at differing wavelengths.

Table 2 [discrete features and zonal winds]

Figure 2 [zonal wind profile]

3.1. Winds at Southern Latitudes

In the southern hemisphere, we see numerous features within the –43° to –50° band that has repeatedly shown many features (Smith et al., 1986; Karkoschka, 1998; Hammel et al., 2001).

These features (2003-P, 2003-B, 2003-Q, 2003-O, 2003-AA, 2003-M, 2003-N, and 2003-R) appear in a hatched region in Fig. 2 and are shaded gray in Table 2. As with earlier HST and Keck observations (Hammel et al., 2001), the zonal velocities within these latitudes match those of Voyager features to within the measurement error.

The two more southerly features, 2003-A and 2003-C, appear to differ slightly from Voyager measurements at their respective latitudes. In the case of 2003-A, this is likely due to the challenge of defining a single position for a large extended feature (see Fig. 1c, columns 1 and 2, for example; see also Fig. 3, in which we show maps of individual features). To within the rather large uncertainty in 2003-A's velocity (based on its positional uncertainty), its motion is consistent with earlier observations. Measurements of 2003-C were hampered because this feature lies on the edge of the bright polar collar. However, it had a concentrated bright core in 2003 (for example, see H-band images in column 1 of Fig. 1b and column 3 of Fig. 1c), thus permitting precise measurements. The agreement with earlier measurements at this latitude is just barely within the errors: we find a velocity of 152 ± 3 m/s at latitude –42.8° ± 0.7°, compared with 161 ± 8 m/s at –43.3° ± 0.4° for feature 2000-7 (Hammel et al., 2001). We conclude that to within our ability to measure the positions of discrete features, the winds in the southern hemisphere have remained constant since the Voyager epoch.

3.2. Equatorial Winds

The only prior information about Uranus wind velocities within ±20° of the equator was a value inferred from the radio occultation experiment on Voyager 2, a velocity of –109 ± 42 m/s at –4.5° ± 2.5° (Lindal et al., 1987). We report here the first direct zonal wind measurements on Uranus at these latitudes.

In our Keck images, features in this latitudinal region fall into two categories: (1) two features relatively far from the equator that are typical of Uranus in size and relative brightness, and (2) features almost directly at the equator that are somewhat atypical. There are two features, in the first category: 2003-D and 2003-E. No features have ever been seen before near 2003-E's latitude (–13°), thus its zonal velocity uniquely constrains the shape of wind profile in that region. In contrast, 2003-D is interesting because its +19.4° ± 1.0° latitude is statistically identical to the +20.6° ± 0.6° latitude of feature 2000-4 (Hammel et al., 2001), yet its velocity of +12 ± 5 m/s is considerably faster than the older measurement of –20 ± 10 m/s. This discrepancy is discussed further in §3.3. Feature 2203-D also has a rather unusual shape (Fig. 3), discussed below in §5.

Figure 3 [Rogues gallery of Uranus features]

The second category of equatorial features, i.e., those seen within ±2° of the equator of Uranus, are atypical of Uranus features in that they are rather large but faint and diffuse ("fuzzy patches"; see maps in Fig. 3). Their indistinct shape makes determining positions for them quite difficult, leading to large uncertainties in velocity. The velocities range from –28 to –78 m/s. To within their errors, the two slowest velocities are consistent with the Voyager equatorial velocity (Lindal et al., 1987), but the bulk of the equatorial measurements—along with the rest of the observed velocities in 2003—suggests that the current equatorial wind speeds are likely faster that the value inferred by Lindal et al. (1987).

Another intriguing aspect of these equatorial features is their relative position in longitude: they are separated by roughly 30° or multiples thereof, and this spacing in constant over the four days of our observations (Fig. 4). Based on (1) their non-standard appearance, (2) their regular, constant spacing, and (3) their roughly similar velocities, we suggest that these features are a

manifestation of an equatorial wave. If one assumes that the spacing is regular at 30° (i.e., that the "missing" patches were simply too faint and diffuse to be recognized), this implies an N=12 pattern.

Figure 4 [Longitudes of equatorial features]

Studies of atmospheric waves on the other outer planets often focus on tracing wave-induced undulations in the location of an edge or a band. Examples include: Saturn's northern mid-latitude ribbon wave (see recent assessment by Sanchez-Lavega, 2002); the north polar hexagon of Saturn (Godfrey, 1988), thought to be an N=6 Rossby wave forced by a nearby anticyclone (Allison et al., 1990); and a latitudinal excursion of Neptune's dark band that was interpreted as an N=1 wave (Sromovsky et al. 2001). However, propagating waves may also manifest themselves as variable cloud opacities or a periodic series of vortices. Studies at thermal wavelengths on Jupiter have revealed patterns of stratospheric features that move slowly with respect to the interior, typically within roughly 20° of the equator (Magalhães et al., 1989, 1990; Orton et al., 1991); IRIS data also showed waves on Saturn (Achterberg and Flasar, 1996). A search for wave manifestations in 5-μm imaging of Jupiter's troposphere yielded a number of plausible candidates (Harrington et al., 1996). Our results would be the first identification of a global-scale atmospheric wave pattern on the planet Uranus.

Some models of convection in planetary interiors suggest a possible link between the dynamics of the (perhaps deep) interior with the stratosphere and upper troposphere via convective cells, which, if strong enough, could act as a forcing mechanism for waves (Hart et al. 1986a, 1986b). Such models are attractive for Uranus because: (1) they are consistent with a pattern of waves that move slowly with respect to the interior, as these equatorial features appear

to do, and (2) long-term observations have indeed shown tandem atmospheric changes over a significant fraction of the atmosphere, from the upper stratosphere down to tens of bars (Hammel and Lockwood 2004). These models also predict coherent patterns of meridionally-aligned features on planetary scales. Such features have in fact been observed on Neptune: sporadically a "bright complex" of features has appeared and remain fixed in relative longitude over many degrees on latitude and many planetary rotations (Hammel et al., 1995; discussed further in Sromovsky et al., 2002). They have not been seen on Uranus, but as the insolation and activity on Uranus become more Neptune-like, we may yet see examples of this class of atmospheric features.

3.3. Winds at Northern Latitudes

As of 2000, the northernmost feature tracked was at +41.6° latitude (Hammel et al., 2001). We report here velocities for six features further north, extending the zonal wind profile up to +47.7° latitude. The zonal velocities show a steady rise as latitudes increase, with one exception, and eventually reach the highest velocity recorded yet on Uranus, 218 ±2 m/s for feature 2003-J at almost +48°. The exception was 2003-F. However, position measurements of this feature were highly uncertain, as demonstrated in the order-of-magnitude larger uncertainty of its velocity: not only was the feature extended in longitude, but two of its three sightings were on the planetary limb.

Our results for the northern mid-latitudes hemisphere are surprising and perhaps the most interesting of all our wind measurements. Above, we mentioned Feature 2003-D, which appears to have a higher velocity than a feature at similar latitude in 2000. In fact, all the features in the Northern hemisphere appear to have higher velocities than similar-latitude counterparts from earlier years. Features 2003-X and 2003-Y (latitudes +27.0° and +27.3°) have velocities of 34 ±

4 and 40± 4 m/s, compared to features 1997-B, 1997-2, and 1997-G (latitudes +27.2°, +27.3°, and +27.4°), with respective velocities of 20 ± 1, 22 ± 2, and 15 ± 1 m/s (Karkoschka, 1998; Hammel et al., 2001). Likewise, feature 2003-V at +36° is moving at 92 ± 7 m/s, in contrast to feature 2000-2's more leisurely pace of 78 ± 2 m/s at the same latitude.

We believe these changes are intrinsic to Uranus, rather than a processing artifact, for several reasons. First, we are using the same analysis techniques and tools used by Hammel et al. (2001). Also, the southern mid-latitude velocities match earlier measurements quite well (§3.1 above). Furthermore, feature 2003-I (latitude +40.9° ± 0.4°, velocity 152 ± 2 m/s) reproduces the latitude and velocity of older feature 2001-1 exactly (latitude +41.6° ± 0.4°, velocity 152 ± 2 m/s), indicating there is not a problem with northern hemispheric measurements. Finally, changes in zonal velocities have been seen in other outer planet wind profiles, for example, Saturn's equatorial jet has slowed (Sánchez-Lavega et al., 2003).

The older velocities at these latitudes "lagged" behind a simple reflection of the southern velocities into the north. This led to the speculation of an asymmetric wind profile (Karkoschka, 1998), but a more northerly feature measured several years later appeared to fall directly on that reflected southern profile (feature 2001-1, latitude +41.6° ± 0.4°, velocity 152 ± 2 m/s), casting the asymmetric model into doubt (Hammel et al., 2001). These newer, faster velocities bring the northern mid-latitude profile closer to alignment with the reflected southern velocities.

4. Atmospheric Symmetry

Hammel and Lockwood (2004) showed that the long-term photometric record of Uranus was dominated by seasonal variation. They also demonstrated that prior to the last solstice, the northern hemisphere of Uranus must have been of comparable brightness to the southern

hemisphere; i.e., an "asymmetric" Uranus was not consistent with the observed photometry (Hammel and Lockwood 2004). Yet all images to date have been asymmetric, showing no bright northern polar collar.

In Fig. 2, we shaded the latitude ranges of both the existing southern polar collar, and the reflective range in the northern hemisphere (i.e., +43° to +50°). Comparison of these shaded regions with the images in Fig. 1 show clearly that no counterpart to the southern polar collar has yet developed in the north. However, not only are there are many discrete features within this northern zone (2003-L, 2003-G, 2003-H, 2003-K, 2003-F, and 2003-J), but they are often extended in longitude (see 2003-F, 2003-G, and 2003-L in Fig. 3), particularly when compared with features of similar brightness in the southern hemisphere. Furthermore, these northern features have the highest velocities yet seen for discrete features on Uranus. The two points may be related.

We speculate that the features seen between +43° and +50° are the nascent northern bright collar. As insolation continues to saturate these latitudes during the seasonal progression on Uranus, the cloud activity could become even more vigorous, resulting in many more bright features and streaks. Eventually such northern streaks could blend to form a bright collar as seen in the south, where only the very brightest feature 2003-C can be discerned individually at the collar's northernmost edge.

5. Detailed Feature Structure

The brightest features show remarkable details in their structure, more reminiscent of the Voyager images of Neptune than of Uranus. Such detail appeared not only for the brightest features, such as 2003-A, but even for fainter features. Feature 2003-N, for example, shows a

persistent arc-like jet (Fig. 3). Similarly, Feature 2003-D has a strange curved shape (Fig. 3), which persists over many rotations.

Readers are cautioned that the relative zonal velocities can often give rise to misleading appearances. For example, before one invokes a divine communication in the striking "cross" feature seen at northern latitudes on 4 Oct (third column of Fig. 1b), one should inspect the earliest set of images on 5 October (first column of Fig. 1c). The feature 2003-W, which was centered directly below 2003-V, has now slipped many degrees in longitude due to its slower velocity. By the end of 6 October, 2003-W is no longer even on the disk when 2003-V is fully visible (column 3 of Fig. 1d). Interestingly, the "arms" of the "cross" maintain their relative position to the bright core of 2003-V, suggesting a dynamical linkage.

Summary

We obtained a series of exquisite near-infrared images of Uranus using the Keck II 10-m telescope in October 2003. The myriad atmospheric details are stunning, and give a glimpse of a planetary atmosphere on the edge of equinox. We studied the zonal winds, the distribution of features and zonal brightness patterns, and are even able to study detailed structure associated with individual features.

We confirm the continued stability of the zonal wind pattern in the southern hemisphere. We report the first direct measurements of zonal winds in the equatorial region, and suggest that the features within a few degrees of the equator are a manifestation of a global-scale atmospheric wave. Features at northern mid latitudes appear to moving at faster velocities that earlier features seen at those latitudes, indicative of dynamic change in the atmosphere on time scales of

just a few years. Features at latitudes northward of +43° show the highest winds seen yet on the planet Uranus, reaching velocities of more than 200 m/s.

Because of its severe obliquity (an axial tilt of 98°) Uranus experiences the most extreme insolation change of any major planet in our solar system, especially during the years surrounding its 2007 equinox. Whether the remarkable details and activity we see now will continue through to equinox, or whether yet more remarkable changes are in store for us as equinox passes, only time and continued observations will tell.

Acknowledgements

HBH acknowledges support for this work from NASA grants NAG5-11961 and NAG5-10451. IdP acknowledges partial support by NSF and the Technology Center for Adaptive Optics, managed by the University of California at Santa Cruz under cooperative agreement No. AST-9876783. SG's work was performed under the auspices of the U.S. Department of Energy, National Nuclear Security Administration, by the University of California, Lawrence Livermore National Laboratory under contract No. W-7405-Eng-48.

We thank the Keck AO staff (especially D. Le Mignant and M. van Dam) for optimizing the AO system for planetary observations. The Keck Observatory is operated as a scientific partnership among the California Institute of Technology, the University of California and NASA. The Observatory was made possible by the generous financial support of the W. M. Keck Foundation. We recognize the significant cultural role of Mauna Kea within the indigenous Hawaiian community, and we appreciate the opportunity to conduct observations from this revered site.

References

Achterberg, R. K., Flasar, F. M. 1996. Planetary-Scale Thermal Waves in Saturn's Upper Troposphere. Icarus 119, 350-369.

Allison M., Godfrey, D. A., Beebe, R. F., 1990. A wave dynamical interpretation of Saturn's polar hexagon. *Science* **247,** 1061–1062.

Allison, M., Beebe, R. F., Conrath, B. J., Hinson, D. P., Ingersoll, A. P. 1991. Uranus atmospheric dynamics and circulation. In *Uranus* (J. T. Bergstralh, E. D. Miner and M. S. Matthews, Ed.), pp. 253-295. Univ. Arizona Press, Tucson.

Davies, M. E., Abalakin, V. K., Bursa, M., Lieske, J. H., Morando, B., Morrison, D., Seidelmann, P. K., Sinclair, A. T., Yallop, B. 1996. Cartographic coordinates and rotational elements of the planets and satellites: 1994. Celest. Mech. Dyn. Astron. 63, 127-148.

Gibbard, S. G., de Pater, I., Hammel, H. B. 2004. Near-infrared adaptive optics imaging of the satellites and individual rings of Uranus from the W. M. Keck Observatory. Submitted to Icarus.

Godfrey, D. A. 1988. A hexagonal feature around Saturn's north pole. *Icarus* **76,** 335–356.

Hammel, H. B., Lockwood, G. W. 2004. Atmospheric Variability on Uranus and Neptune: Seasonal, Solar-Driven, or Stochastic? Submitted to Icarus.

Hammel, H. B., Lockwood, G. W., Mills, J. R., Barnet, C. D. 1995. Hubble Space Telescope Imaging of Neptune's Cloud Structure in 1994. *Science* **268**, 1740.

Hammel, H. B., Rages, K., Lockwood, G. W., Karkoschka, E., de Pater, I. 2001. New measurements of the winds of Uranus. Icarus 153, 229-235.

Harrington, J. 1994. *Planetary Infrared Observations: the occultation of 28 Sagittarii by Saturn and the dynamics of Jupiter's atmosphere*. Doctoral thesis in planetary science, MIT.

Harrington, J., Dowling, T. E., Baron, R. L. 1996. Jupiter's tropospheric thermal emission. Icarus 124, 32-44.

Hart, J. E., Glatzmaier, G. A., Toomre, J. 1986a. Space-laboratory and numerical simulations of thermal convection in a rotating hemispherical shell with radial gravity. Journal of Fluid Mechanics 173, 519-544.

Hart, J. E., Toomre, J., Deane, A. E., Hurlburt, N. E., Glatzmaier, G. A., Fichtl, G. H., Leslie, F., Fowlis, W. W., Gilman, P. A. 1986b. Laboratory Experiments on Planetary and Stellar Convection Performed on Spacelab 3. Science 234, 61-64.

Karkoschka, E. 1998. Clouds of high contrast on Uranus. Science 280, 570-572.

Lindal, G. F., Lyons, J. R., Sweetnam, D. N., Eshleman, V. R., Hinson, D. P., Tyler, G. L. 1987. The atmosphere of Uranus: Results of radio occultation measurements with Voyager 2. Journal Geophys. Res. 92, 14987-15001.

Magalhães, J. A., Weir, A. L., Gierasch, P. J., Conrath, B. J., Leroy, S. S. 1990. Zonal motion and structure in Jupiter's upper troposphere from Voyager infrared and imaging observations. Icarus 88, 39-72.

Magalhães, J. A., Weir, A. L., Conrath, B. J., Gierasch, P. J., Leroy, S. S. 1989. Slowly moving thermal features on Jupiter. Nature 337, 444-447.

Ness, N. F., Acuña, M. H., Behannon, K. W., Burlaga, L. F. Connerney, J. E. P., Lepping, R. P., Neubauer, F. M. 1986. Magnetic fields at Uranus. Science 233, 85-89.

Orton, G. S., and 14 colleagues 1991. Thermal maps of Jupiter - Spatial organization and time dependence of stratospheric temperatures, 1980 to 1990. Science 252, 537-542.

Rages, K. A., Hammel, H. B., Friedson, A. J. (2004). Evidence for Seasonal Change at Uranus' South Pole. Submitted to Icarus.

Sánchez-Lavega, A. 2002 Observations of Saturn's ribbon wave 14 years after its discovery. Icarus 158, 272-275.

Sánchez-Lavega, A., Pérez-Hoyos, S., Rojas, J. F., Hueso, R., French, R. G. 2003. A strong decrease in Saturn's equatorial jet at cloud level. Nature 423, 623-625.

Smith, B. A., Soderblom, L. A., Beebe, R. F., Bliss, D., Boyce, J., Brahic, A., Briggs, G. A., Brown, R. H., Collins, S. A., Cook II, A., F., Croft, S. K., Cuzzi, J., Danielson, G. E., Davies, M. E., Dowling, T., Godfrey, D., Hansen, C. J., Harris, C., Hunt, G. E., Ingersoll, A. P., Johnson, T. V., Krauss, R. J., Mazursky, H., Mitchell, J. L., Morrison, D., Owen, T., Plescia, J. B., Pollack, J. B., Porco, C. C., Rages, K., Sagan, C., Shoemaker, E., Sromovsky, L. A., Stoker, C., Strom, R. G., Suomi, V. E., Synnot, S. P., Terrile, R. J., Thomas, P., Thompson, W. R. Veverka, J. 1986. Voyager 2 in the Uranian system: Imaging science results. Science 233, 43-64.

Sromovsky, L. A., Fry, P. M., Dowling, T. E., Baines, K. H., Limaye, S. S. 2001. Coordinated 1996 HST and IRTF imaging of Neptune and Triton III. Neptune's atmospheric circulation and cloud structure. Icarus 149, 459-488.

Sromovsky, L. A., Fry, P. M., Baines, K. H., 2002. The unusual dynamics of northern dark spots on Neptune. Icarus 156, 16-36.

Warwick, J. W., Evans, D. R., Romig, J. H., Sawyer, C. B., Desch, M. D., Kaiser, M. L., Alexander, J. K., Carr, T. D., Staelin, D. H., Gulkis, S., Poynter, R. L., Aubier, M., Boischot, A., Leblanc, Y., Lecacheux, A., Pederson, B. M., Zarka, P. 1986. Voyager 2 radio observations of Uranus. Science 233, 102-106.

Table 1

Uranus Atmosphere Observations in 2003

Date	Set	UT*	Filter	Exp †
3 Oct	1	5:36	J	5 x 60
		5:22	H	5 x 60
		5:53	Kp	6 x 120
	2	9:09	J	5 x 60
		9:32	H	5 x 60
		9:40	Kp	5 x 120
4 Oct	1	5:18	J	3 x 60
		5:03	H	3 x 60
		5:24	Kp	3 x 120
	2	7:24	J	3 x 60
		7:03	H	3 x 60
		7:28	Kp	3 x 120
	3	9:55	J	3 x 60
		9:39	H	3 x 60
		10:01	Kp	3 x 120
5 Oct	1	5:18	J	3 x 60
		5:02	H	3 x 60
		5:22	Kp	3 x 120
	2	7:20	J	3 x 60
		7:00	H	3 x 60
		7:28	Kp	3 x 120
	3	9:33	J	3 x 60
		9:19, 9:38	H	3 x 60, 1 x 300
		9:59, 10:05	Kp	1 x 300, 1 x 60
6 Oct	1	5:35	J	3 x 60
		5:20	H	3 x 60
		5:40	Kp	3 x 120
	2	6:56	J	3 x 60
		7:11	H	3 x 60
		7:17	Kp	3 x 60
	3	9:53	J	2 x 60
		9:58, 10:02, 10:09	H	1 x 60, 1 x 60, 1 x 60
		9:07, 9:18, 10:06, 10:08	Kp	1 x 300, 1 x 300, 1 x 60, 1 x 60

* We typically show the start time, to the nearest minute, for the first exposure at each filter; for non-standard sequences, start times for each image are listed.

† This is “number of images” x “exposure time in seconds”.

Table 2

Zonal Winds of Uranus in 2003 from Discrete Features *

Feature	Latitude (°)	Period (hrs)	Velocity (m/s)
2003-J	47.7 ± 0.6	15.26 ± 0.02	218 ± [illegible]
2003-F	47.1 ± 0.9	15.58 ± 0.35	181 ± 42
2003-K	46.1 ± 0.8	15.40 ± 0.02	207 ± [illegible]
2003-H	43.9 ± 0.8	15.58 ± 0.05	192 ± [illegible]
2003-G	43.3 ± 0.8	15.72 ± 0.03	177 ± [illegible]
2003-L	43.5 ± 0.4	15.74 ± 0.05	173 ± [illegible]
2003-I	40.9 ± 0.4	15.96 ± 0.02	152 ± [illegible]
2003-V	35.5 ± 1.6	16.50 ± 0.05	92 ± [illegible]
2003-Y	27.3 ± 1.2	16.94 ± 0.03	40 ± [illegible]
2003-X	27.0 ± 1.2	16.99 ± 0.03	34 ± [illegible]
2003-W	24.6 ± 1.5	17.11 ± 0.10	17 ± 14
2003-Z	24.0 ± 1.0	17.08 ± 0.02	22 ± [illegible]
2003-D	19.4 ± 1.0	17.15 ± 0.04	12 ± [illegible]
2003-BB	2.1 ± 2.3	17.43 ± 0.18	–28 ± 27
2003-U	2.4 ± 1.3	17.60 ± 0.05	–53 ± [illegible]
2003-T	2.0 ± 0.6	17.52 ± 0.04	–41 ± [illegible]
2003-S	1.7 ± 0.3	17.72 ± 0.16	–70 ± 23
2003-CC	0.7 ± 1.2	17.55 ± 0.05	–46 ± [illegible]
2003-DD	0.7 ± 0.8	17.77 ± 0.08	–78 ± 11
2003-E	–13.7 ± 0.7	17.41 ± 0.03	–25 ± [illegible]
2003-P	–23.3 ± 0.9	17.05 ± 0.03	26 ± [illegible]
2003-B	–25.2 ± 0.7	16.99 ± 0.03	34 ± [illegible]
2003-Q	–25.6 ± 0.8	16.96 ± 0.03	37 ± [illegible]
2003-O	–27.0 ± 0.5	16.90 ± 0.01	45 ± [illegible]
2003-AA	–28.6 ± 0.8	16.88 ± 0.04	47 ± [illegible]
2003-M	–30.7 ± 0.4	16.76 ± 0.01	63 ± [illegible]
2003-N	–31.0 ± 0.6	16.67 ± 0.04	75 ± [illegible]
2003-R	–31.5 ± 0.8	16.71 ± 0.04	69 ± [illegible]
2003-A	–37.7 ± 0.7	16.18 ± 0.13	131 ± 17
2003-C	–42.8 ± 0.7	15.93 ± 0.03	152 ± [illegible]

Gray rows correspond to hatched areas in Fig. 2.

FIGURE CAPTIONS

Fig. 1. Uranus in 2003. The four panels show representative images of Uranus from 3-6 October UT. Each column represents one set of images. We show only one image per filter per set; typically three images were obtained at each wavelength (see Table 1). The top row is a schematic in which the tracked features are labeled (occasionally a feature can be seen that does not have a label; this indicates either it was seen only once or identification was ambiguous on other nights). The next three rows are J, H, and Kp, respectively. Note that the times are not always sequential from top to bottom. In most Kp images, the rings dominate the image, though features W, V, X, and Y are easily detected. The rings are also easily seen at H, and usually at J (see Gibbard et al. 2004 for further ring discussion). The fainter or more diffuse features are difficult to see in these stretches optimized for the full planet disk; we used stretches with greater contrast for feature measurement. (a) 3 October 2003; note that only two sets were obtained this night. (b) 4 October 2003. (c) 5 October 2003. (d) 6 October 2003.

Fig. 2. Uranus Zonal Wind Profile in 2003. Solid squares are the points listed in Table 2; open symbols are past measurements from HST, Keck, and Voyager (see Table II in Hammel et al. 2001). The 2003 letter labels are typically offset by +50 m/s in velocity, with an occasional larger value to avoid overlapping letters. The large error bars on the 2003 equatorial features are indicative of their diffuse nature, which makes defining their locations challenging. To within the measurement errors, they have similar zonal velocities, and in fact may be a manifestation of a wave pattern (see discussion in §3). The hatched region from –50° to –43° corresponds to the bright polar collar clearly evident at J and H (Fig. 1). The hatched region from +43° to +50° mirrors the southern latitudes values. Many of northern features are clustered at these latitudes (see "symmetry" discussion in §4). The hatched region from –32° to –23° was defined to

enclose most of the southern mid-latitude features seen in the 2003 data and the earlier measurements. The symmetric band in the north, from +23° to +32°, encloses many of the northern features. The lines represent various models: thin solid – non-weighted fit to Voyager data (Allison et al. 1991); dotted - asymmetric model of Karkoschka (1998); thick solid – fit to overall data set (see §3).

Fig. 3. Maps of Individual Features in 2003. Maps of each tracked feature used for zonal wind measurements demonstrate the diversity of feature sizes, shapes, and contrasts in 2003. Each map is 30° in longitude and 15° in latitude, with north up and east to the left. The figure is organized schematically by latitude so that comparison with Fig. 2 can be made; the hatched areas are the same as is Fig. 2. Each map is stretched separately, thus faint features (T, B) look similar to bright features (A, V) in these maps. Actual relative feature brightnesses can be determined from the images in Fig. 1. We generally used maps when features were isolated (far from other features), but some images do contain multiple features and rings (Z, D).

Fig. 4. Longitudes of Equatorial Features. The longitudes of the six identified equatorial features are shown as a function of 2003 day of year (DOY 276 = 3 October 2003); each curve is labeled with the 2003 feature name from Table 2 (feature 2003-T is shown twice, the second time with 360° added). Measured points are marked with a plain asterisk; longitudes that were interpolated or extrapolated are marked with a boxed asterisk; the interpolation/extrapolation slope was the feature drift rate (°/day) used to calculate the velocities shown in Table 2. Across the top of the figure, the mean difference in longitude between one feature and the next is shown. The delta value is the average of all four nights (including interpolated or extrapolated values). Most delta values are roughly 30° or multiples thereof, suggesting a wave pattern.

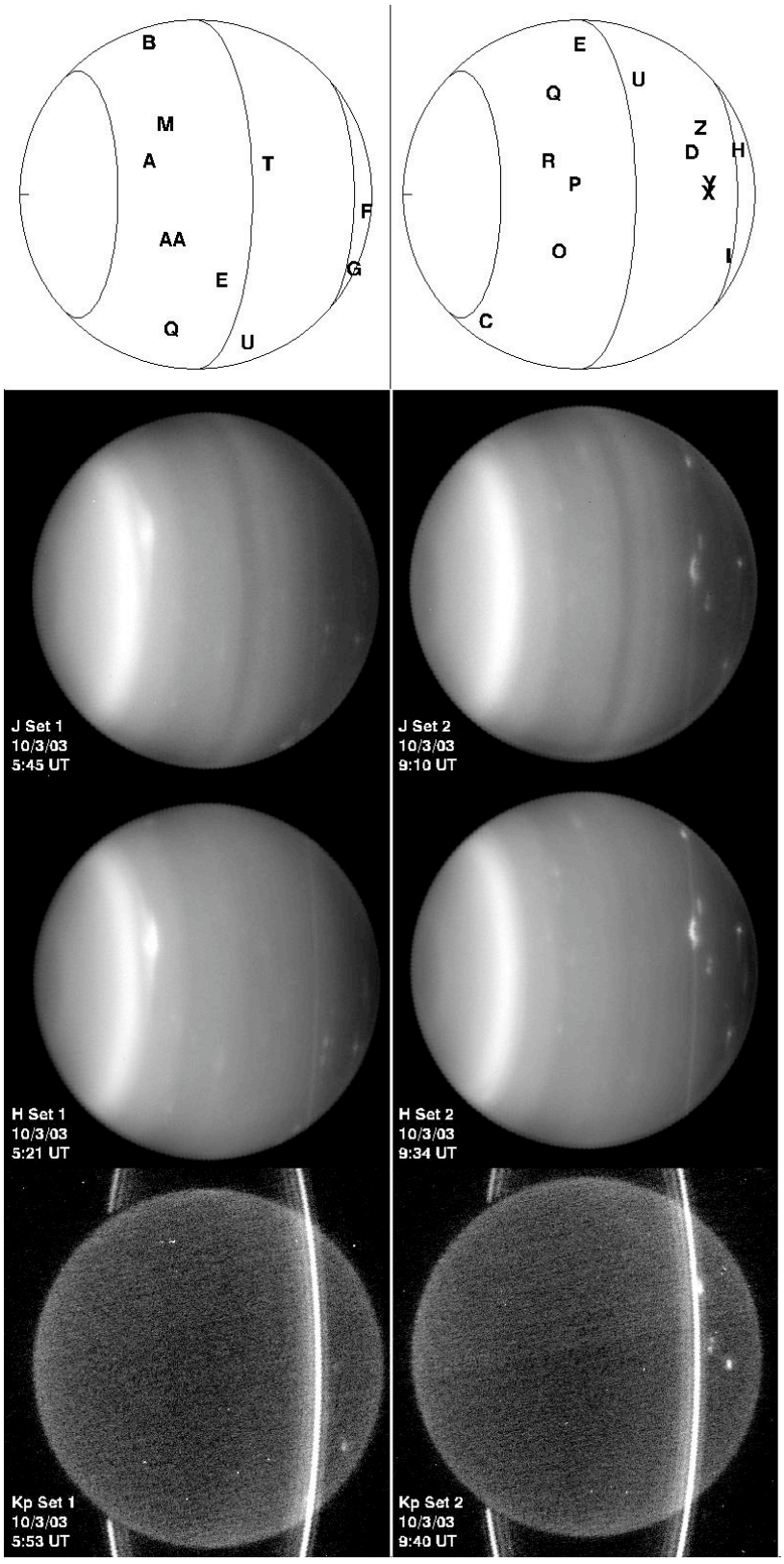
B
M
A
T
F
AA
G
E
Q
U
E
U
Q
Z
D
H
R
P
O
I
C
J Set 1
10/3/03
5:45 UT
J Set 2
10/3/03
9:10 UT
H Set 1
10/3/03
5:21 UT
H Set 2
10/3/03
9:34 UT
Kp Set 1
10/3/03
5:53 UT
Kp Set 2
10/3/03
9:40 UT

FIGURE 1a

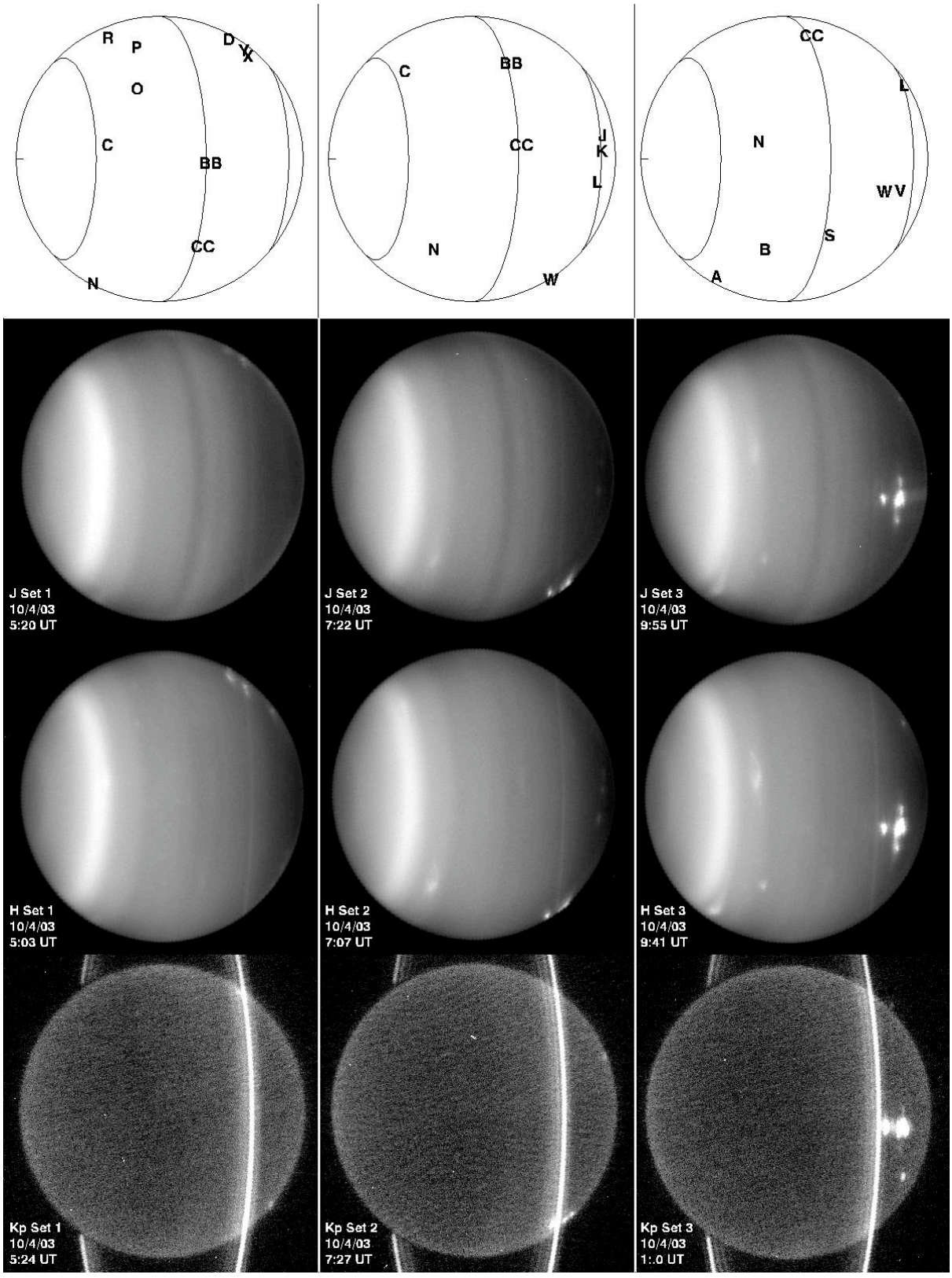
R
P
D
Y
X
O
C
BB
CC
N
C
BB
CC
J
K
L
N
W
CC
L
N
W V
S
B
A
J Set 1
10/4/03
5:20 UT
J Set 2
10/4/03
7:22 UT
J Set 3
10/4/03
9:55 UT
H Set 1
10/4/03
5:03 UT
H Set 2
10/4/03
7:07 UT
H Set 3
10/4/03
9:41 UT
Kp Set 1
10/4/03
5:24 UT
Kp Set 2
10/4/03
7:27 UT
Kp Set 3
10/4/03
1:.0 UT

FIGURE 1b

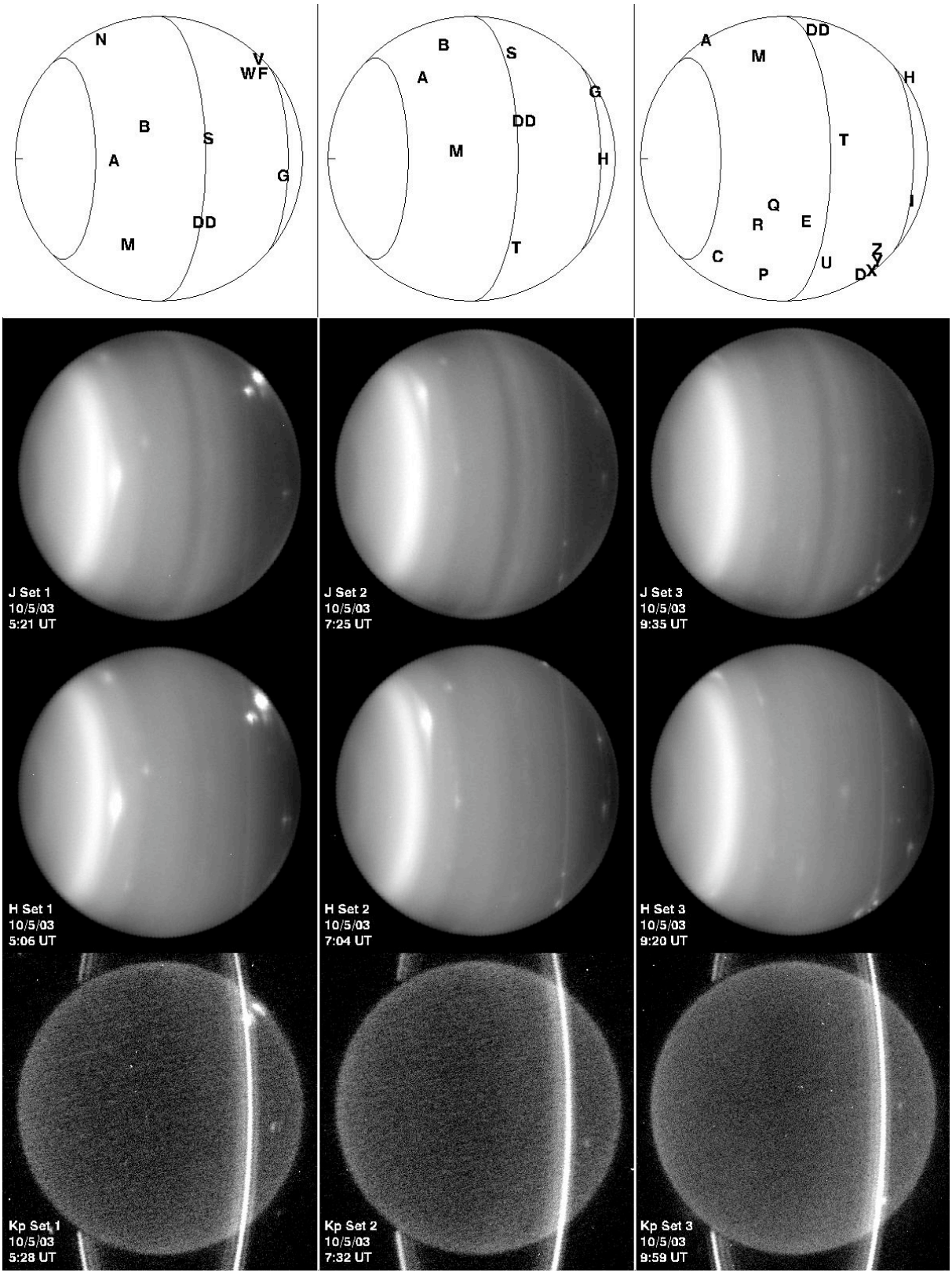
N
V
WF
B
S
A
G
DD
M
B
S
A
G
DD
M
H
T
A
DD
M
H
T
Q
R
E
J
C
P
U
Z
X
D
J Set 1
10/5/03
5:21 UT
J Set 2
10/5/03
7:25 UT
J Set 3
10/5/03
9:35 UT
H Set 1
10/5/03
5:06 UT
H Set 2
10/5/03
7:04 UT
H Set 3
10/5/03
9:20 UT
Kp Set 1
10/5/03
5:28 UT
Kp Set 2
10/5/03
7:32 UT
Kp Set 3
10/5/03
9:59 UT

FIGURE 1c

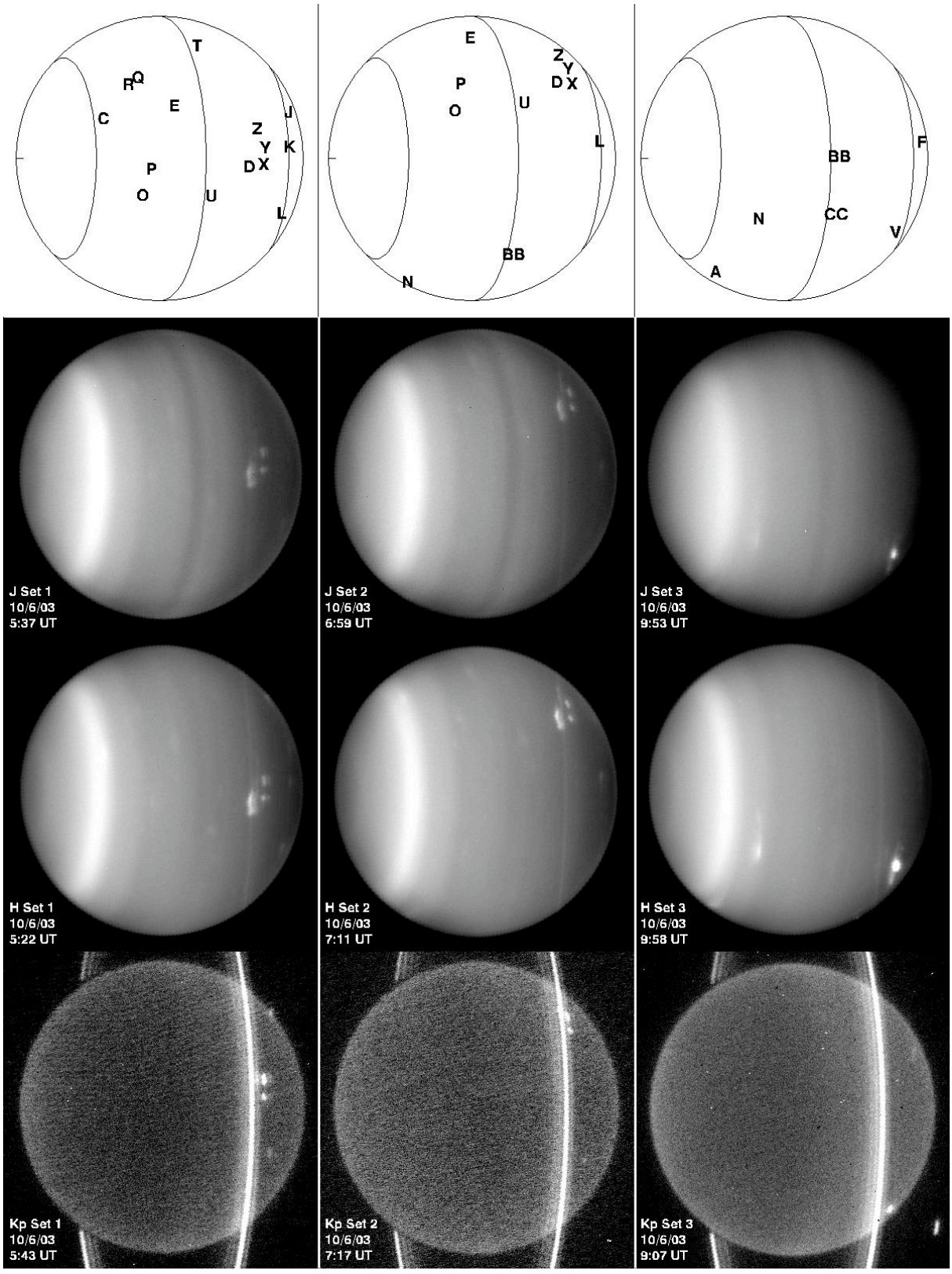
T
Q
R
E
C
J
Z
Y
K
D
X
P
O
U
L
E
Z
Y
P
D
X
O
U
L
BB
N
F
BB
N
CC
V
A
J Set 1
10/6/03
5:37 UT
J Set 2
10/6/03
6:59 UT
J Set 3
10/6/03
9:53 UT
H Set 1
10/6/03
5:22 UT
H Set 2
10/6/03
7:11 UT
H Set 3
10/6/03
9:58 UT
Kp Set 1
10/6/03
5:43 UT
Kp Set 2
10/6/03
7:17 UT
Kp Set 3
10/6/03
9:07 UT

FIGURE 1d

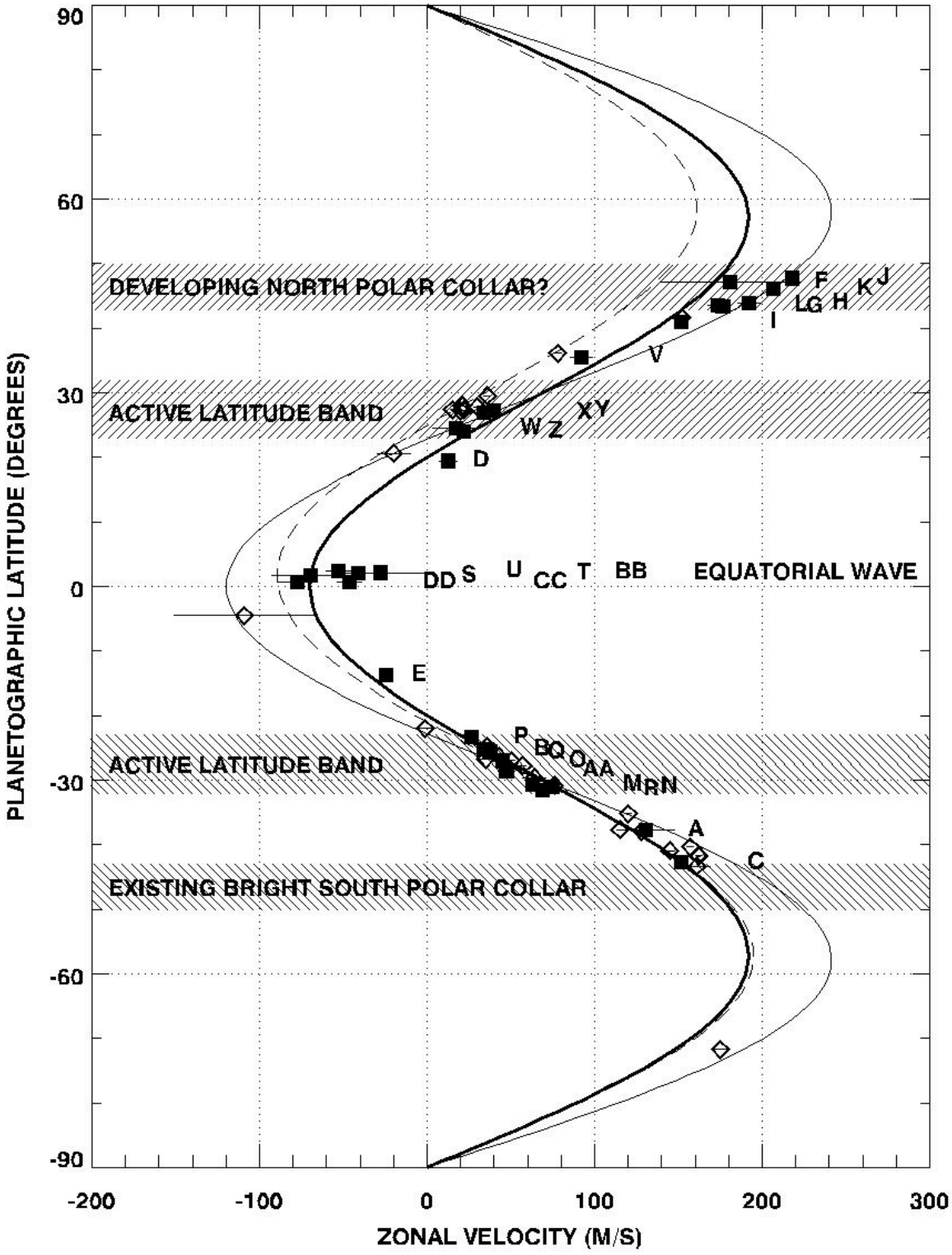
90
60
30
0
-30
-60
-90
-200
-100
0
100
200
300
PLANETOGRAPHIC LATITUDE (DEGREES)
ZONAL VELOCITY (M/S)
DEVELOPING NORTH POLAR COLLAR?
ACTIVE LATITUDE BAND
ACTIVE LATITUDE BAND
EXISTING BRIGHT SOUTH POLAR COLLAR
EQUATORIAL WAVE
F
K
J
LG
H
I
V
XY
W
Z
D
DD
S
U
CC
T
BB
E
P
BQ
O
AA
M
R
N
A
C

FIGURE 2

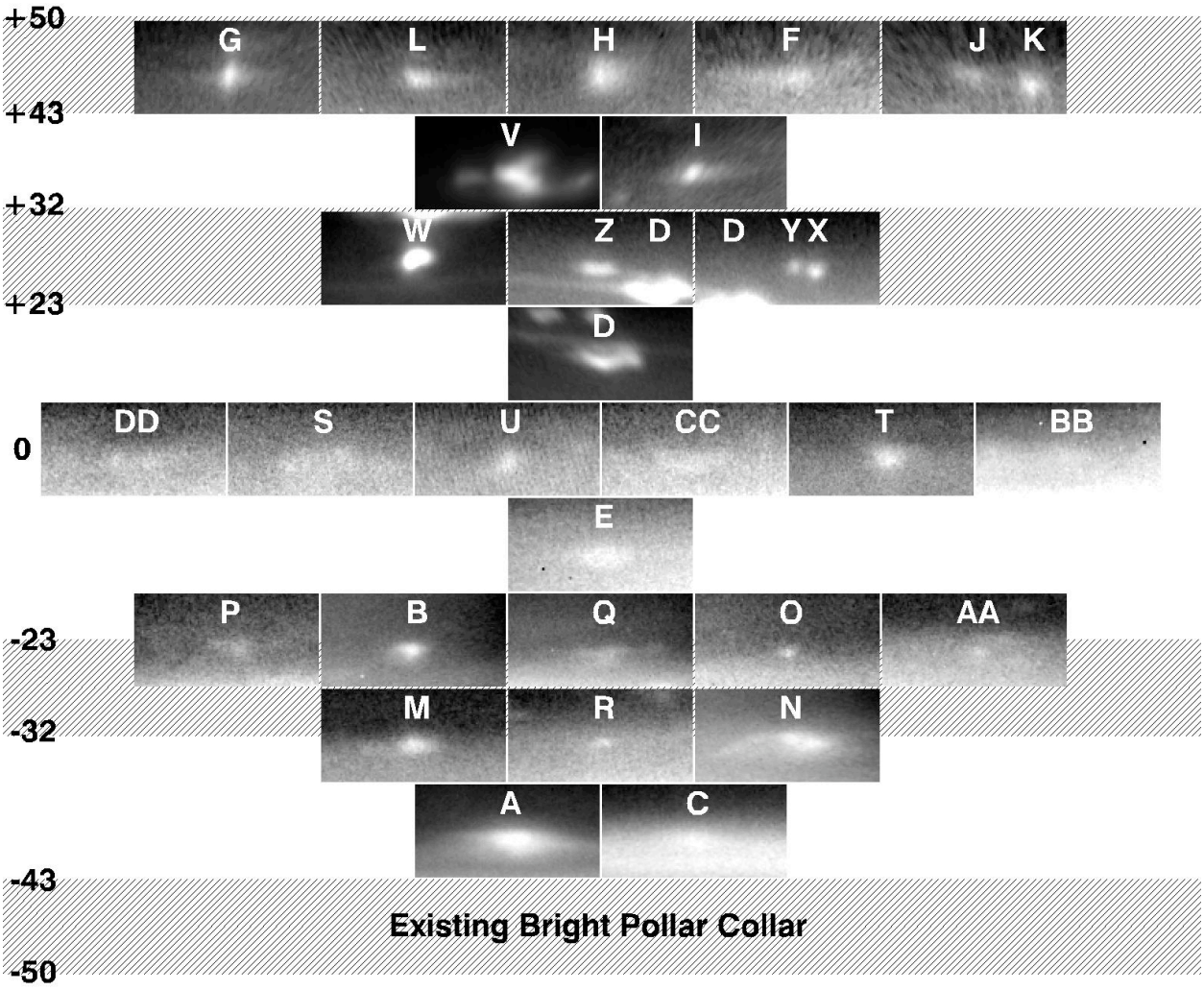
+50
+43
+32
+23
0
-23
-32
-43
-50
G
L
H
F
J K
V
I
W
Z D
D YX
D
DD
S
U
CC
T
BB
E
P
B
Q
O
AA
M
R
N
A
C
Existing Bright Pollar Collar

FIGURE 3

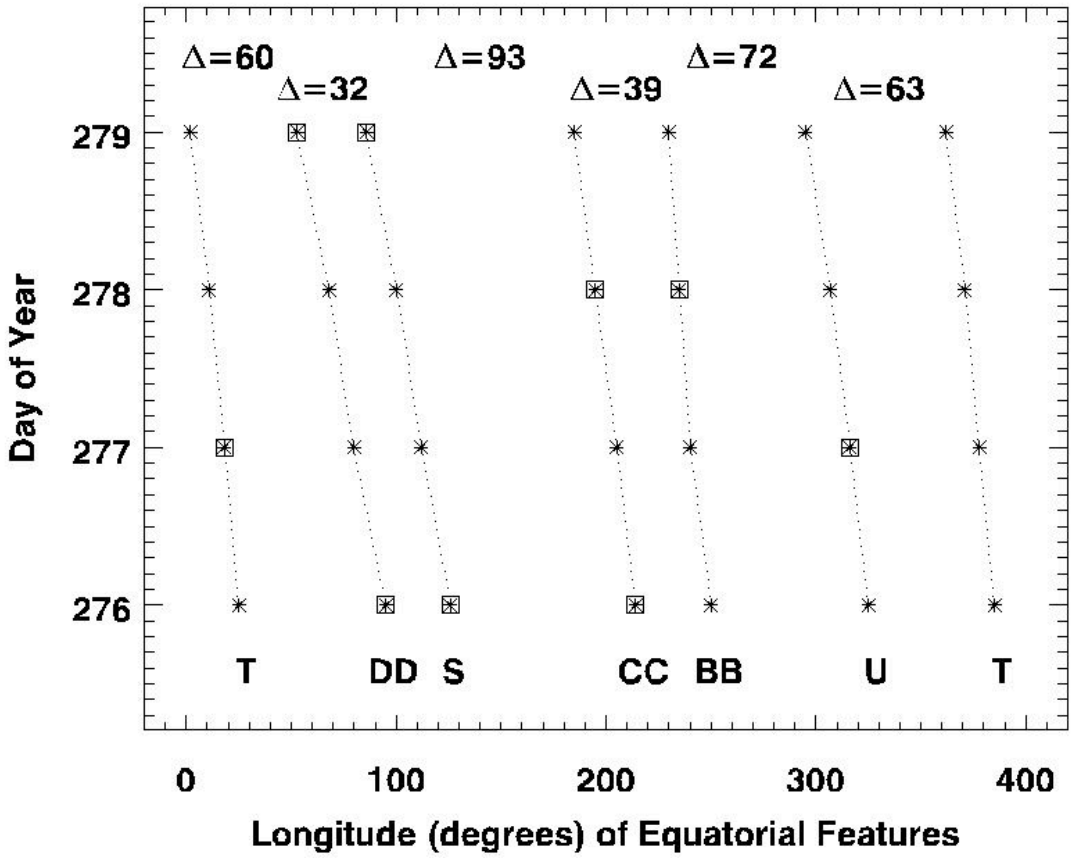
Δ=60
Δ=32
Δ=93
Δ=39
Δ=72
Δ=63
279
278
277
276
Day of Year
T
DD
S
CC
BB
U
T
0
100
200
300
400
Longitude (degrees) of Equatorial Features

FIGURE 4